

Enhanced soft magnetic properties of SiO_2-coated FeSiCr magnetic powder cores by particle size effect

Mingyue Ge(葛铭悦), Likang Xiao(肖礼康), Xiaoru Liu(刘潇如), Lin Pan(潘嶙), Zhangyang Zhou(周章洋), Jianghe La(蓝江河), Zhengwei Xiong(熊政伟), Jichuan Wu(吴冀川), and Zhipeng Gao(高志鹏)

Citation: Chin. Phys. B, 2024, 33 (**10**): 107503. DOI: 10.1088/1674-1056/ad6556
Journal homepage: http://cpb.iphy.ac.cn; http://iopscience.iop.org/cpb

What follows is a list of articles you may be interested in

Dzyaloshinskii-Moriya interaction and field-free sub-10 nm topological magnetism in Fe/bismuth oxychalcogenides heterostructures

Yaoyuan Wang(王垚元), Long You(游龙), Kai Chang(常凯), and Hongxin Yang(杨洪新)
Chin. Phys. B, 2024, 33 (**9**): 097508. DOI: 10.1088/1674-1056/ad6a0e

Alternating spin splitting of electronic and magnon bands in two-dimensional altermagnetic materials

Qian Wang(王乾), Da-Wei Wu(邬大为), Guang-Hua Guo(郭光华), Meng-Qiu Long(龙孟秋), and Yun-Peng Wang(王云鹏)
Chin. Phys. B, 2024, 33 (**9**): 097507. DOI: 10.1088/1674-1056/ad6425

Magnetic domain structures in ultrathin $Bi_2Te_3/CrTe_2$ heterostructures

Tirui Xia(夏体瑞), Xiaotian Yang(杨笑天), Yifan Zhang(张逸凡), Xinqi Liu(刘馨琪), Xinyu Cai(蔡新雨), Chang Liu(刘畅), Qi Yao(姚岐), Xufeng Kou(寇煦丰), and Wenbo Wang(王文波)
Chin. Phys. B, 2024, 33 (**8**): 087504. DOI: 10.1088/1674-1056/ad4a3a

Frequency combs based on magnon-skyrmion interaction in magnetic nanotubes

Tijjani Abdulrazak, Xuejuan Liu(刘雪娟), Zhejunyu Jin(金哲珺雨), Yunshan Cao(曹云姗), and Peng Yan(严鹏)
Chin. Phys. B, 2024, 33 (**8**): 087503. DOI: 10.1088/1674-1056/ad4ff5

Critical behavior of quasi-two-dimensional ferromagnet $Cr_{1.04}Te_2$

Wei Niu(钮伟), Qin-Xin Song(宋沁心), Shi-Qi Chang(常世琦), Min Wang(王敏), Kui Yuan(袁奎), Jia-Cheng Gao(高嘉程), Shuo Wang(王硕), Zhen-Dong Wang(王振东), Kai-Fei Liu(刘凯斐), Ping Liu(刘萍), Yong-Bing Xu(徐永兵), Xiao-Qian Zhang(张晓倩), and Yong Pu(普勇)
Chin. Phys. B, 2024, 33 (**7**): 077506. DOI: 10.1088/1674-1056/ad4cd8

Enhanced soft magnetic properties of SiO_2-coated FeSiCr magnetic powder cores by particle size effect

Mingyue Ge(葛铭悦)[1], Likang Xiao(肖礼康)[2], Xiaoru Liu(刘潇如)[1], Lin Pan(潘嶙)[3], Zhangyang Zhou(周章洋)[3], Jianghe Lan(蓝江河)[2], Zhengwei Xiong(熊政伟)[1,4,†], Jichuan Wu(吴冀川)[3,‡], and Zhipeng Gao(高志鹏)[1,3,§]

[1] *Joint Laboratory for Extreme Conditions Matter Properties, School of Mathematics and Physics, Southwest University of Science and Technology, Mianyang* 621010, *China*
[2] *Southwest Institute of Applied Magnetism, Mianyang* 621010, *China*
[3] *Institute of Fluid Physics, China Academy of Engineering Physics, Mianyang* 621900, *China*
[4] *Sichuan Civil-military Integration Institute, Mianyang* 621010, *China*

(Received 9 May 2024; revised manuscript received 2 July 2024; accepted manuscript online 19 July 2024)

It has been known that metal FeSiCr powders with large average particle sizes have been typically employed to prepare magnetic powder cores (SMCs), with few studies reported on the influence of magnetic properties for original powders with various average particle sizes less than 10 μm. In this work, SiO_2-coated FeSiCr SMCs with different small particle sizes were synthesized using the sol–gel process. The contribution of SiO_2 coating amount and voids to the soft magnetic properties was elaborated. The mechanism was revealed such that smaller particle sizes with less voids could be beneficial for reducing core loss in the SMCs. By optimizing the core structure, permeability and magnetic loss of 26 and 262 kW/cm^3 at 100 kHz and 50 mT were achieved at a particle size of 4.8 μm and ethyl orthosilicate addition of 0.1 mL/g. The best DC stacking performance, reaching 87%, was observed at an ethyl orthosilicate addition rate of 0.25 mL/g under 100 Oe. Compared to other soft magnetic composites (SMCs), the FeSiCr/SiO_2 SMCs exhibit significantly reduced magnetic loss. It further reduces the magnetic loss of the powder core, providing a new strategy for applications of SMCs at high frequencies.

Keywords: FeSiCr, SiO_2, size effect, magnetic properties, DC superposition

PACS: 75.47.Np **DOI:** 10.1088/1674-1056/ad6556

1. Introduction

Metallic soft magnetic composites are known for their high effective permeability (μ_{eff}), low coercion (H_C), and minimal residual magnetic induction, therefore have a wide range of uses in areas such as city power supply.[1,2] FeSiCr soft magnetic powder cores (SMCs) exhibit high Curie temperature and saturation magnetization. Compared to pure iron powder cores, addition of Si and Cr elements provides them with higher temperature stability, better DC superposition characteristics, lower power losses, and resistance to aging.[3,4] However, conventional all-metal magnetic powder core materials face challenges associated with low resistivity, frequency instability, and performance deterioration at increased temperatures, thereby limiting their utilization in applications. Typically, coating the surface of FeSiCr SMCs with an insulation layer can effectively increase the electrical resistivity and reduce the losses.[5,6] These composites can be categorized based on the cladding material into organic and inorganic coatings, with inorganic coatings offering more superior thermal stability and insulation properties relative to the organic counterparts.[7–15] As a representative inorganic material, SiO_2 is easy to synthesize with a low melting point, which is advantageous for forming a uniform glassy coating during annealing. Thus, SiO_2-coated FeSiCr SMCs were favored by many researchers.[16,17]

So far, a number of researchers have studied the variations in magnetic properties of soft magnetic powder core materials at a fixed particle size. For instance, Yu *et al.* employed the sol–gel method to fabricate FeSiCr/SiO_2 SMCs with an average particle size of 8 μm, achieving a maximum density of 6.2–5.8 g/cm^3 and a minimum magnetic loss of 418.32 kW/cm^3.[16] Li and his team prepared FeSiCr/SiO_2 SMCs with an average particle size of 10.3 μm and obtained a minimum magnetic loss of 493.3 kW/cm^3.[17] Despite using the same raw material and coating method, previous FeSiCr/SiO_2 SMCs with various average particle sizes all exhibited void defects, which led to different degrees of magnetic loss deterioration. Moreover, studies on other iron-based SMCs with different particle sizes have also been reported.[18–20] Zhou *et al.* examined the effect of powder size on the magnetic properties of FeSiBC SMCs with three particle sizes (20–90 μm) using water atomized FeSiCr powders and found that smaller particle sizes reduced voids and decreased magnetic losses to 239.15 mW/cm^3.[18] Woo *et al.* revealed that FeSiCrB SMCs with the smallest particle size (25 μm) possessed the optimal void structure and loss re-

†Corresponding author. E-mail: zw-xiong@swust.edu.cn
‡Corresponding author. E-mail: junhuawu123@sina.cn
§Corresponding author. E-mail: z.p.gao@foxmail.com

© 2024 Chinese Physical Society and IOP Publishing Ltd

duction achieved.[19] Dirk conducted theoretical calculations to analyze the impact of particle sizes on the effective initial magnetic permeability, showing that the void structures in the SMCs were decreased, and the magnetic properties were improved as the particle size decreased from 500 μm to 63 μm.[20] From these earlier results,[16–20] it could be inferred that smaller particle sizes were advantageous for enhancing the magnetic performance of SMCs. However, most research has typically employed metal powders with larger average particle sizes, with fewer studies reporting on the influence of magnetic properties for original powders with an average particle size less than 10 μm. Unfortunately, FeSiCr-based SMCs with different particle sizes less than 10 μm have been rarely fabricated, and the effect of such smaller FeSiCr particle sizes with SiO_2 insulation coating on SMCs magnetic properties remains unexplored to date.

In this work, FeSiCr/SiO_2 SMCs were prepared by using the sol–gel method. The differences in magnetic performance between two different particle sizes of FeSiCr SMCs are compared. The coating thickness of the samples is modified by adjusting the amount of tetraethyl orthosilicate (TEOS). The sample's magnetic properties as well as the DC, hysteresis loss and eddy current loss are studied systematically.

2. Experimental procedure

2.1. Sample preparation

Two FeSiCr powders with different average particle sizes, labeled as S1 and S2, were prepared using the casting method. The experimental schematic is shown in Fig. 1. As a coupling agent and silicon source, silane coupling agent ($C_9H_{23}NO_3Si$, APTES, Chron Chemicals) and tetraethyl orthosilicate ($C_8H_{20}O_4Si$, TEOS, Chron Chemicals) were employed, respectively. FeSiCr powder (20 g) was used with 170 mL of absolute ethanol and placed in a water bath. A mixture of 5 mL of APTES and 30 mL of deionized water was then added to the solution, and the mixture was maintained under mechanical stirring at 500 rpm for one hour. Following the APTES reaction for one hour at room temperature, TEOS was added (0 mL/g, 0.05 mL/g, 0.1 mL/g, 0.15 mL/g, 0.2 mL/g, and 0.25 mL/g), and the temperature was further raised to 60 ℃. After heating the solution for two hours, FeSiCr /SiO_2 powder was obtained. The coated powder was dried at 60 ℃ for 24 hours. Epoxy resin (1 wt%) was dissolved in acetone, then the coated powder was added and stirred until the acetone was evaporated. As a lubricant, 0.5 wt% zinc stearate was added to the coated powder before pressing. The powder mixture was pressed into an annular sample with an outer diameter of 12.8 mm and an inner diameter of 6.4 mm under a pressure of 1950 MPa. Following annealing at 600 ℃ for two hours in a vacuum atmosphere, the sample was cooled in the furnace.

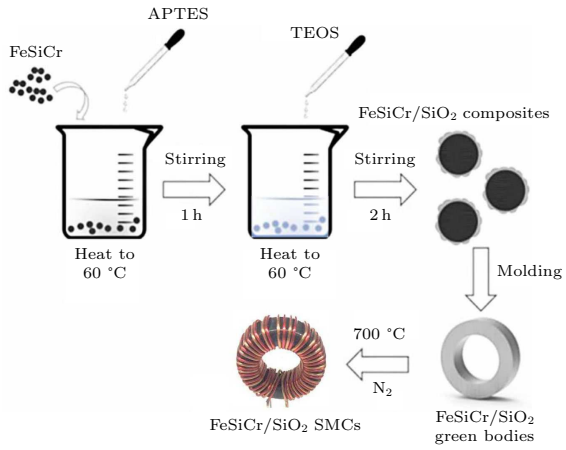


Fig. 1. Schematic diagram of the experimental setup.

2.2. Dissipation of losses

Losses were tested using a *B*–*H* analyzer to measure the total loss of samples. To investigate the response mechanism of insulation-coated SiO_2 to reduce eddy current losses, we performed loss separation of the total losses to obtain the corresponding different types of losses. The total losses (P_{cv}) can be expressed as[21,22]

$$P_{cv} = P_h + P_e + P_{ex}, \tag{1}$$

$$P_h = f \oint H \, dB, \tag{2}$$

$$P_e = \frac{CB^2 f^2 d^2}{\rho}, \tag{3}$$

where P_h is the hysteresis loss, f is the frequency, H is the magnetic field, and B is the magnetic induction, P_e is the eddy current loss, C is the proportionality constant, B is the flux density, ρ is the resistivity, and d is the thickness of SMCs.

Based on the above equations, the power loss can be expressed as

$$\frac{P_{cv}}{f} = \frac{P_h}{f} + \frac{P_e}{f} + \frac{P_{ex}}{f}, \tag{4}$$

$$\frac{P_{cv}}{f} = C_h + C_e f + \frac{P_{ex}}{f}, \tag{5}$$

where C_h and C_e are two constants. Thus, P_h is proportional to f, P_e is proportional to f^2, P_{ex} is often negligible. Therefore, we can fit a P_{cv}/f vs. f curve linearly. The intercept and slope in the P_{cv}/f vs. f curve are C_h and C_e.

Thus, P_h and P_e can be calculated according to the following equations:

$$P_h = C_h f, \tag{6}$$

$$P_e = C_e f^2. \tag{7}$$

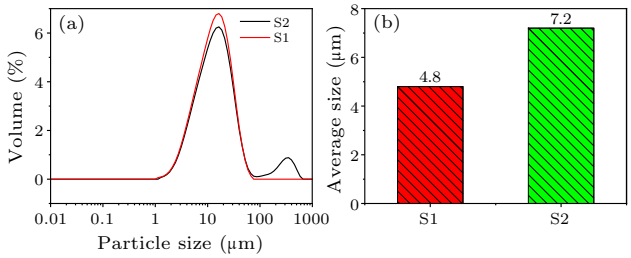


Fig. 2. (a) Particle size distribution and (b) average size of different types of FeSiCr powders.

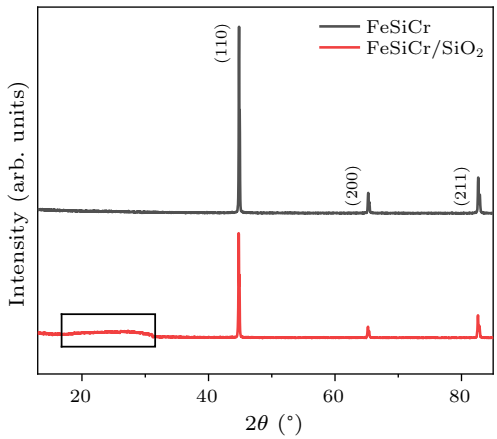


Fig. 3. XRD of powders.

2.3. Material characterization

Particle size analysis was conducted by employing a laser particle size analyzer (Malvern Rasterizer 3000). The microstructure of the FeSiCr/SiO_2 powder cores was examined via scanning electron microscopy (SEM, TM4000, Hitachi). To characterize the silica insulating coating, energy dispersive spectroscopy (EDS) elemental mapping was employed. The resistivity of the powder cores was assessed using a four-probe resistance tester (RTS-8). The density of SMCs was determined using the density balance. The AC magnetic properties of the samples were evaluated utilizing a *B*–*H* curve analyzer (SY-8218, Iwatsu) across a frequency range of 10–100 kHz, with a *B* value of 50 mT. Furthermore, the DC superposition characteristics of the powder cores were investigated by employing a TH1776 DC bias current source. The TH1776 DC bias current source was employed to measure the inductance (L) of SMCs without magnetic field as L_0. The L/L_0 characterizes the reduction of inductance with applied magnetic field, the larger the L/L_0 the better the DC bias performance.

3. Results and discussion

Figure 2 shows the particle size distribution of the two FeSiCr powders. According to the data in Fig. 2(a), the average particle size of the two powders can be calculated using the formula[23]

$$D[p,q] = \frac{\sum_{i=1}^{n} D_{i,\mathrm{v}}^{p}}{\sum_{i=1}^{n} D_{i,\mathrm{v}}^{q}}, \tag{8}$$

where i represents the i-th column in the histogram, there are a total of n columns in the figure. D_i represents the geometric mean of the particle size of the i-th column, which is the square root of the upper particle size times the lower particle size. As a result, the average particle sizes of S1- and S2-type FeSiCr powders are 4.8 μm and 7.2 μm, respectively.

As shown in Fig. 3, only three diffraction peaks of the Fe phase with the simple cubic structure can be observed in the XRD pattern of pure Fe powders without SiO_2 coating. By comparison, after SiO_2 coating, in addition to the three diffraction peaks of the Fe phase, a "round hump" appears at $2\theta = 15°$–$30°$, indicating that the coated SiO_2 is amorphous phase.

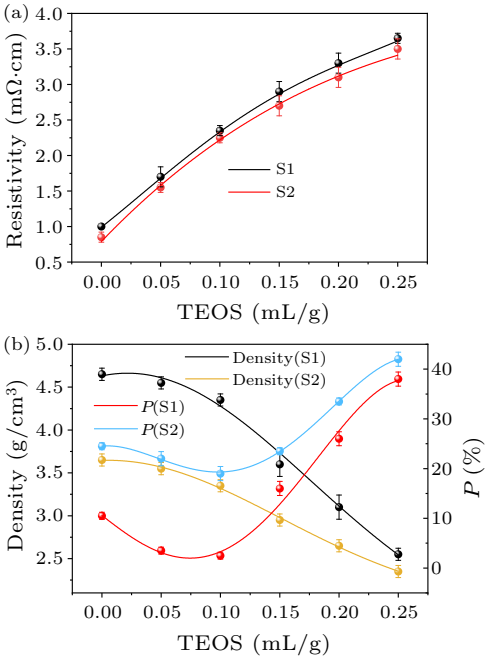


Fig. 4. Effect of the addition of TEOS on (a) resistivity, (b) density and P of the FeSiCr/SiO_2 SMCs at $B = 50$ mT and $f = 100$ kHz.

Figures 4(a) and 4(b) present the electrical resistivity and density of FeSiCr/SiO_2 SMCs prepared with different TEOS addition amounts. As the number of cladding increases, the resistivity increases, indicating that more SiO_2 formation leads to an increase in the insulating properties of the SMCs. Also, the values of resistivity of S1 and S2 are close to each other, indicating the close amount of SiO_2 cladding [Fig. 4(a)]. For comparison, we tested the average particle size of pure FeSiCr and SiO_2-coated FeSiCr powders using a laser particle sizer. As shown in Fig. S3 of supplementary material, the average particle sizes of SMCs with the TEOS amounts of 0 mL/g, 0.1 mL/g, and 0.2 mL/g are 4.8 μm, 13.6 μm, and 18.8 μm, respectively. Obviously, the particle size of FeSiCr powders increases with the TEOS amount, which can be attributed to the increase of silica coating thickness derived from TEOS hydrolysis. The result has also been demonstrated that the increase of TEOS contents induces the thicker silica coating in previous works on SiO_2-coated Fe-based SMCs using the

sol–gel method.[16,17] The more insulating SiO_2 shell on the FeSiCr core induces the increased resistivity, which is a direct inducement to reduce the eddy currents (P_e).[10] The density of SMC increases gradually with the increase of TEOS contents [Fig. 4(b)], which is related to the number of voids. The void rate (P) can be calculated by the formula

$$P = 1 - \frac{\rho_0}{x\rho_{\mathrm{FeSiCr}} + (1-x)\rho_{\mathrm{SiO_2}}}, \tag{9}$$

where ρ_0 represents the actual density of FeSiCr/SiO_2 SMCs; ρ_{FeSiCr} [Fig. 4(b)] denotes the measured density of FeSiCr SMCs without coating (4.6 g/cm^3), while $\rho_{\mathrm{SiO_2}}$ signifies the theoretical density of SiO_2 (2.6 g/cm^3), x is the mass fraction. Noteworthily, with a relatively lower TEOS content, the decline degree of density is smaller than that of larger contents. Correspondingly, the P shows two different trends, displaying that the P decreases at first and then increases with the increase of TEOS contents. There are two types of structural changes in SMCs: the first is the increase of SiO_2 thickness. This results in a decrease in the overall density of SMCs since the atomic mass fraction of SiO_2 is significantly lower than that of FeSiCr. The second type is the void variation. With a lower amount of SiO_2 coating, the void tends to decrease. It indirectly suggests that a thin SiO_2 coating can better maintain the integrity of the SMCs' sphericalshell structure, thereby enhancing their overall magnetic properties. In contrast, as the amount of SiO_2 coating increases, the P becomes significantly greater in company with the more pronounced downward trend of densities. The overuse of TEOS causes the shedding of the SiO_2 layer [Fig. 4(b)]. The resulting heterogeneous cladding structures generate more voids. Therefore, the P first decreases and then increases, with a minimum of 2% at TEOS of 0.1 mL/g. From 0 mL/g to 0.1 mL/g TEOS contents, the decrease of P for S1- and S2-type SMCs is 8% and 6%, while the increasing P of S1- and S2-type SMCs is 36% and 23% from 0.1 mL/g to 0.25 mL/g, respectively. Obviously, the changed degree of P in the S1-type SMCs is greater than that of S2. Thus, smaller particle size of SMCs has higher densities and lower voids.

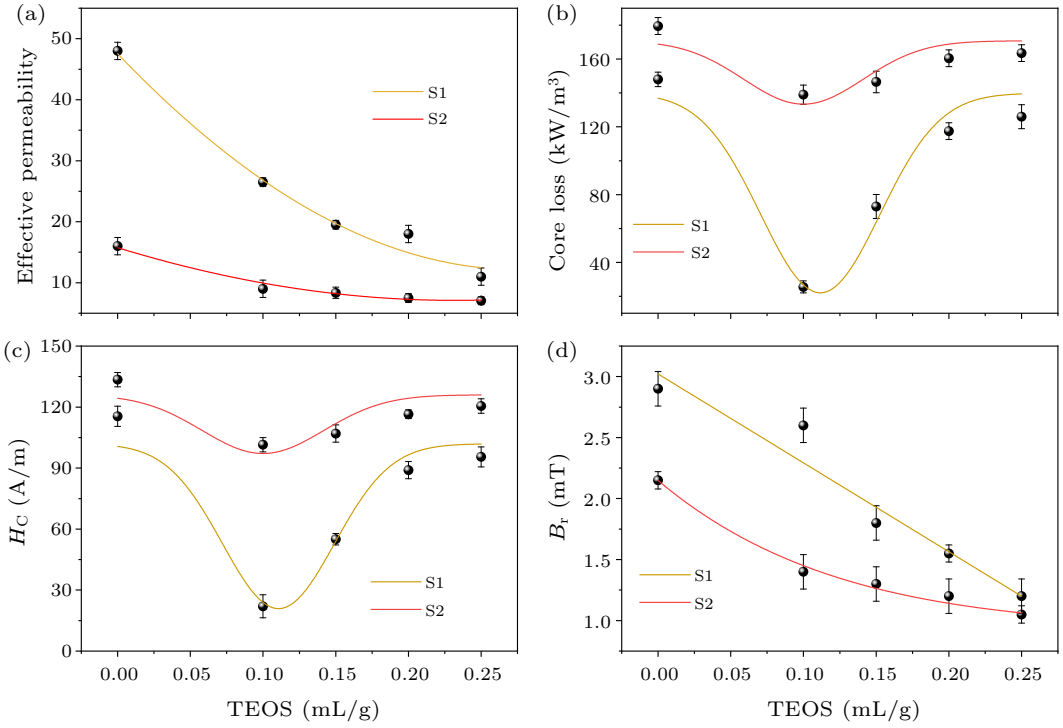


Fig. 5. Comparison of magnetic properties of S1 and S2 types of FeSiCr/SiO_2 SMCs on (a) μ_{eff}, (b) P_{cv}, (c) H_C, (d) B_r at $f = 10$ kHz and $B = 50$ mT.

Figure 5 shows noteworthy distinctions in the magnetic properties between the S1- and S2-type SMCs, employing identical preparation conditions. For the S1-type SMCs, the μ_{eff} is notably higher than those of the S2-type SMCs, and the μ_{eff} decreases with the addition of TEOS [Fig. 5(a)]. In the uncoated case, the μ_{eff} of S1 is much larger than that of S2, because the non-magnetic voids of S1 are less than that of S2 [Fig. 4(b)]. With the increase of TEOS contents, the SiO_2 coatings with larger average particle sizes are more likely to drop off (Fig. S2 in supplementary material), because the SiO_2-coated FeSiCr powder particles with larger average particle sizes have the greater contact areas. In this case, the adhesion of SiO_2 shell on the larger FeSiCr particles is weaker, making the coating easier to drop off under high-pressure compression. After the SiO_2 coatings drop off, the FeSiCr particles are exposed, consequently inducing that the μ_{eff} decreases more slowly. Compared to the S2-type FeSiCr/SiO_2 SMCs, the S1-type core exhibits a smaller core loss (P_{cv}) [Fig. 5(b)],

lower coercivity (H_C) [Fig. 5(c)], and greater remanence (B_r) [Fig. 5(d)]. This is due to the fact that smaller sized particles have less voids, resulting in a weaker pinning effect, making the smaller H_C and P_{cv} of S1. The more voids mean the lower magnetism. Thus, the B_r of S1 is greater than that of S2. As shown in Figs. 5(b)–5(d), with the increase of TEOS addition, the P_{cv} and H_C of SMCs are both decreased, and then increased, while the B_r is decreased. Overall, the S2-type SMCs have a lower degree of variability in P_{cv}, H_C and B_r than that of S1. The increase of voids and the contents of non-magnetic SiO_2 act to anchor the domain walls, which in turn require additional energy to achieve the same magnetization or demagnetization processes, thereby increasing the H_C.[24] On the contrary, the decreased voids could induce the reduction of H_C. As a result, the H_C is correspondingly decreased and then increased [Fig. 5(c)]. The magnitude of change in H_C of S1 is larger than that of S2 because of the large change in the void of S1 (Fig. 4). The increase of non-magnetic SiO_2 could further result in the decrease of B_r [Fig. 5(d)], meaning the weakening of magnetic properties. The magnitudes of changes in H_C and B_r of S1 are larger than those of S2 because of the greater changes in the void of S1 (Fig. 4).

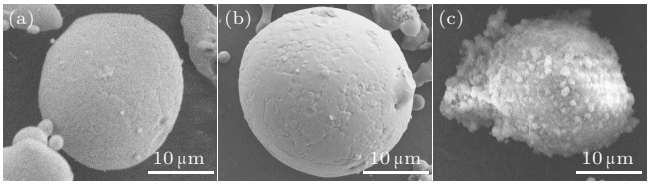


Fig. 6. SEM images of S1-type FeSiCr powder particles with different TEOS amounts of (a) 0 mL/g, (b) 0.1 mL/g, and (c) 0.25 mL/g.

Based on the superior magnetic properties, the S1 type of FeSiCr powders are adopted to investigate the coating process on its magnetic performance. The magnetic loss mechanism is further analyzed in the following. Figure 6 displays the surface morphologies for the S1-type FeSiCr powders coated with different TEOS amounts. From Fig. 6(a), pure FeSiCr powder presents an obvious spherical structure. As the coating amount increases, the insulating coating layer progressively builds up. A uniform layer of coating is formed on the outer surface of the FeSiCr particles [Fig. 6(b)]. The Si and O elements are uniformly distributed on the surface of the FeSiCr particles (Fig. S1). In combination with XRD analysis, the coated SiO_2 is demonstrated to exhibit amorphous state (Fig. 3). Therefore, we can conclude that the amorphous SiO_2 coating is uniformly clad on the crystalline FeSiCr particles. With further increase of TEOS amount, the coating layer on the outer surface of FeSiCr particles starts to exhibit flocculent matter, as seen in Fig. 6(c).

As shown in Fig. 7(a), the annealed S1-type SMCs exhibit a complete spherical structure as the TEOS coating amount is 0.1 mL/g. In Fig. 7(b), with increasing the coating amount to 0.25 mL/g, excessive SiO_2 coating leads to partial coating layer detachment, resulting in an incomplete spherical shell structure of the SMCs. Further elemental analysis of the incomplete coating layer (Fig. S2) indicates the presence of only Si and O elements, suggesting that the excessive SiO_2 coating is unfavorable for the formation of the complete sphericalshell structure in SMCs, which may influence the magnetic performance.

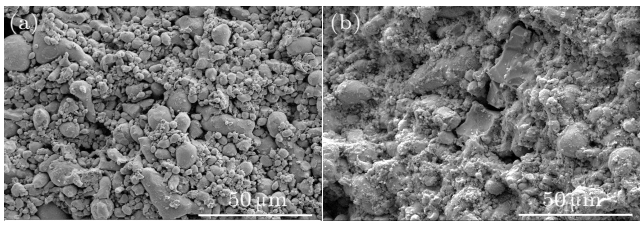


Fig. 7. SEM images of samples after high temperature annealing of S1-type SMCs with (a) 0.1 mL/g and (b) 0.25 mL/g.

Since the P_{cv} of the SCMs are primarily composed of P_h and P_e, we further divide the P_{cv} into P_e and P_h to investigate the influence of the coating process on the SMCs losses.[10,23] Figure 8 illustrates the soft magnetic performance of FeSiCr/SiO_2 SMCs. In Fig. 8(a), it can be observed that the μ_{eff} remains nearly constant with varying frequencies. The P_{cv} [Fig. 8(b)], P_h [Fig. 8(c)], and P_e [Fig. 8(d)] all increase with an increase of frequencies. With an increase of TEOS addition, the μ_{eff} decreases [Fig. 8(a)], owning to the increase of the non-magnetic SiO_2 contents within the SMCs. In Fig. 8(b), the P_{cv} shows a trend of decreasing first and then increasing with changes of TEOS addition.

Figure 9 gives the magnetic loss as a function of TEOS addition. The S1-type SMCs with the smaller particle size have lower P_{cv}, P_e and P_h than those of S2-type SMCs. The resistivities of S1 and S2 are comparable [Fig. 4(a)], so the difference in P_e is not significant, demonstrating the close amount of SiO_2 coating on the particle surface with different sizes. The P_e decreases with the increase of TEOS amount. The more non-magnetic SiO_2 content increases the resistivity and thus reduces P_e.[23] The P_e does not change obviously, which might attribute to the thinner cladding layer relative to the large particles. The P_h for S1-type SMCs is smaller than that of S2, because the P of S1 is less than S2 [Fig. 4(b)], resulting in a more pronounced pinning effect for the S2. Overall, the P_h plays a dominant role in the P_{cv}, inducing that the total P_{cv} of S1 is less than that of S2. Notably, increasing the amount of TEOS results in a decrease of P_h initially, followed by an increase (Fig. 9). The P_h refers to the energy consumed during the repeated magnetization process of ferromagnetic materials due to the magnetic hysteresis. These losses are primarily caused by the pinning effect of domain walls during the magnetization process.[25] With the increase of TEOS contents, the voids first decrease and then increase [Fig. 4(b)]. During the magnetization process, the P can act as pinning centers for domain walls,

impeding the movement of domains. Consequently, the H_C first decreases and then increases, leading to a similar trend in the P_h, which initially decreases and then increases. The addition of the coating layer could fill the voids, making the denser structure and reduced P. Later, with the overuse of the TEOS contents, the coating layer is broken [Fig. 7(b)], forming the heterogeneous sphericalshell structure with the larger P. In the smaller particlesize SMCs, the less voids signify that the same amount of SiO_2 is more likely to fill the voids, presenting the more obvious variations of voids in the S1-type SMCs. Therefore, smaller particle sizes with less voids are beneficial for reducing P_{cv} in the SMCs. As the TEOS coating increases, the P_h dominates the P_{cv}, causing the P_{cv} to first decreases and then increases.

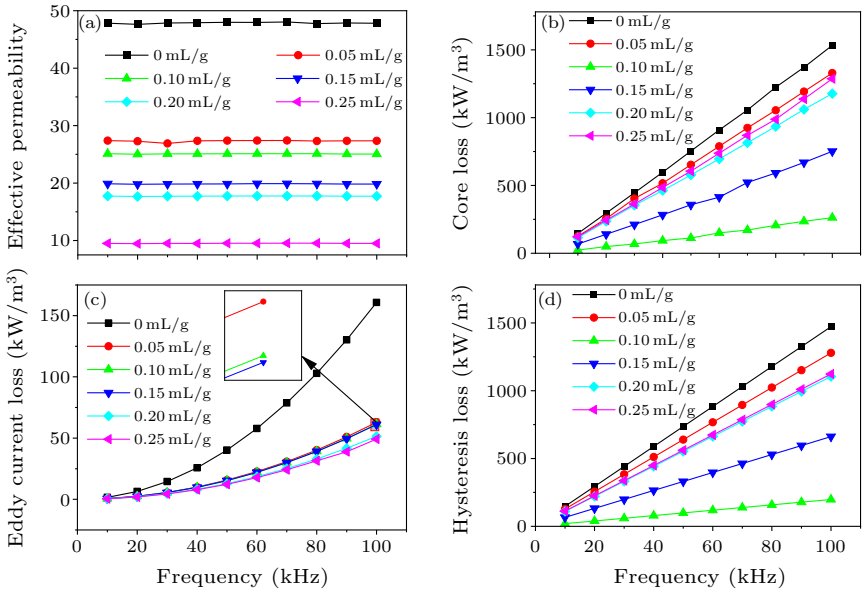


Fig. 8. Effect of the addition of TEOS on AC magnetic properties of the FeSiCr/SiO_2 SMCs on (a) μ_{eff}, (b) P_{cv}, (c) P_h, (d) P_e at various f and $B = 50$ mT. The inset in (c) shows a decrease of P_e as TEOS addition increases from 0.05 mL/g to 0.15 mL/g.

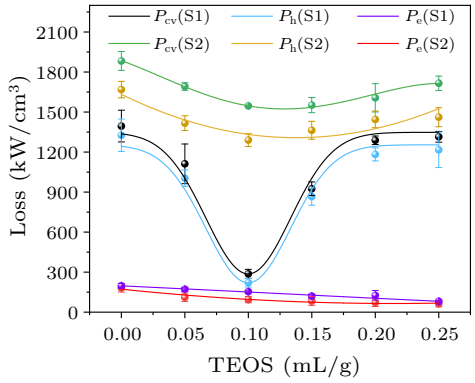


Fig. 9. Magnetic loss of FeSiCr/SiO_2 SMCs on P_{cv}, P_h, and P_e at $B = 50$ mT and $f = 100$ kHz with TEOS additions.

After optimizing the insulation coating processes, the magnetic performance of the FeSiCr/SiO_2 SMC reaches its optimum at $B = 50$ mT and $f = 100$ kHz, with a μ_{eff} of 26 and P_{cv} of 262 kW/m^3. Table 1 provides a comparison of the effective permeability and losses of different types of soft magnetic composite materials. Researchers previously prepared FeSiCr SMCs with four particle sizes of 820 μm, which were obtained as the μ_{eff} of 16.3–45.52 and P_{cv} of 239–1500 kW/m^3 at a magnetic field of 50 mT and a frequency of 100 kHz.[16–18,26,27] Geng *et al.* reported FeSi/ZrO_2 SMCs (45 μm), with a P_{cv} of 489 kW/m^3 ($B = 50$ mT and $f = 50$ kHz).[28] Lei *et al.* fabricated Fe/Al_2O_3 SMCs (70 μm), resulting in a μ_{eff} of 35 and P_{cv} of 400–500 kW/m^3 ($B = 20$ mT and $f = 100$ kHz).[29] Wang *et al.* prepared FeSiCr/$CaCO_3$ SMCs (40 μm), achieving a μ_{eff} of 27 and P_{cv} of 466.5 kW/m^3 ($B = 50$ mT and $f = 100$ kHz).[30] Our FeSiCr/SiO_2 SMCs have relatively higher μ_{eff} of 26 and lower P_{cv} of 262 kW/m^3 at $B = 50$ mT and $f = 100$ kHz under the same test conditions, making the SMCs more conducive to device applications.

Figure 10 shows a comparison of the magnetic performance among the FeSiCr/SiO_2 SMCs produced in this study and currently available commercial FeSi-based SMCs. Compared to the FeSi-based SMCs with a size of 0.356 cm^3 produced by Beijing Seven Star Flight Electronics Co., Ltd. (SSFE), the FeSiCr/SiO_2 SMCs prepared in this study has a slightly lower μ_{eff} (56%), surprisingly companying with a significantly lower P_{cv} (62%).[31] Relative to the Magnetics (MAG) in U.S.A. (size 222 mm^3) and Chang Sung Corporation (CSC) in South Korea (size 14.048 cm^3), our SMCs shows lower μ_{eff} (56%) and reduced P_{cv}, with decreases of 62% and 71%, respectively.[32,33] In comparison to the FeSi-based SMCs with a size of 0.356 cm^3 prepared by Zhejiang Dongmu Keda Magnetics & Electronics Co., Ltd. (KDM), the SiO_2-coated FeSiCr SMCs prepared here has the same μ_{eff} of 26 and reduced P_{cv} by 47%.[34] Therefore, the FeSiCr/SiO_2 SMCs developed in this work have lower losses and are expected to be a valuable resource for domestic applications of SMCs at high frequencies.

Table 1. Comparison of magnetic properties of different soft magnetic materials.

SMCs	Particle size (μm)	50 kHz		100 kHz		B (mT)	References
		μ_{eff}	P_{cv} (kW/m^3)	μ_{eff}	P_{cv} (kW/m^3)		
FeSiCr/SiO_2 (S1)	4.8	26	112	26	262	50	this work
FeSiCr/SiO_2 (S2)	7.2	7.9	881	8	1542		
FeSiCr/SiO_2	8			45.52	418.32	50	[16]
FeSiCr/SiO_2	11			4	493.3	5	[17]
FeSiBC	2			18	239.15	5	[18]
FeSiCr/MgO	14			24	433.55	50	[26]
FeSiCr/PA6	10			16.3	1500	50	[27]
Fe/Al_2O_3	70			35	400-500	20	[29]
FeSiCr/$CaCO_3$	60			27	466.5	100	[30]

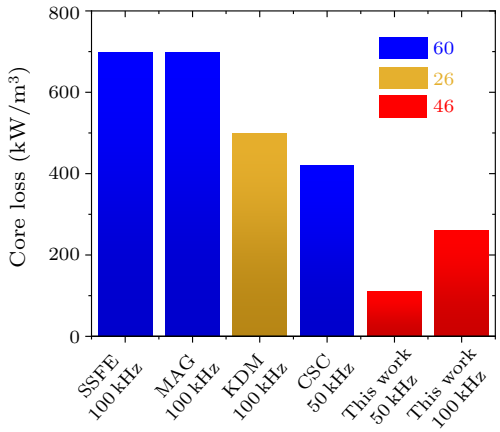


Fig. 10. Magnetic properties of FeSiCr/SiO_2 SMCs produced in this study compared with commercial FeSi-based SMCs.

The presence of a DC component in an AC power system can lead to a decay in L, which is called the DC bias performance.[35,36] Compared to the FeSiBNbCu/ZrO_2 SMCs prepared by Zhou *et al.* with a DC bias performance of 59.3% at 100 Oe, our SMCs have a comparable P_{cv} and better DC bias performance (65%) at the same initial permeability. Therefore, the FeSiCr/SiO_2 SMCs could meet the requirements of relatively low P_{cv} and high DC bias performance, indicating a good application prospect for power magnetic devices.

4. Conclusions

The FeSiCr/SiO_2 powder cores were prepared using the solgel method. Suitable TEOS amount was added to produce the SiO_2 coating outside the FeSiCr particles to form a core-shell structure, while the overuse of TEOS caused the shedding of the SiO_2 layer. The influence of magnetic SMCs properties for original FeSiCr powders with different particle sizes less than 10 μm is explored. During the process of SMCs synthesis, the cooperative effect of the SiO_2 coating and voids on the soft magnetic properties of SMCs is revealed. With the increase of TEOS contents, the slight increase of SiO_2 thickness relative to the micron-sized particles induces the weak variations of resistivity and eddy current loss. In addition, the voids are first decreased and then increased. With a lower amount of SiO_2 coating, the voids tend to decrease, suggesting that a thin SiO_2 coating could well maintain the integrity of the SMCs' spherical-shell structure, thereby enhancing their overall magnetic properties. More SiO_2 coating induces the greater voids in company with the more pronounced downward trend of densities. The fluctuation of voids generates the consistent variations of coercion, hysteresis loss and total loss, which first decrease and then increase. By contrast, the voids are more important and are related to the SiO_2 coating thickness, playing a major role of hysteresis loss in the total loss. Using the smaller particle sizes could be capable of decreasing the voids, further reducing core loss in the SMCs. According to the coating optimization, we achieve μ_{eff} and P_{cv} of 26 and 262 kW/cm^3, respectively, at 100 kHz and 50 mT for the SMCs. Under identical preparation conditions, our SMCs exhibit enhanced DC stacking performance, reaching up to 87%. By adopting the strategy of smaller FeSiCr particle sizes, the soft magnetic properties and DC bias superposition characteristics of FeSiCr/SiO_2 SMCs are significantly improved.

Acknowledgments

This work was supported by the National Natural Science Foundation of China (Grant Nos. U2230119 and U23A20567), 2022 Central Guidance on Local Science and Technology Development Projects (Grant No. 2022ZYDF073), and Outstanding Youth Fund of Sichuan Province (Grant No. 22JCQN0005).

References

[1] Silveyra J M, Ferrara E, Huber D L and Monso T C 2018 *Science* **362** eaao0195
[2] Gutfleisch O, Willard M A, Brück E, Chen C H, Sanker S and Liu J P 2011 *Adv. Mater.* **23** 821
[3] Long J, Ding W and Yang Y 2013 *Corrosion Sci.* **201** 110303
[4] Zhou T D, Tang J K and Wang Z Y 2010 *J. Magn. Magn. Mater.* **322** 2589
[5] Chen S F, Chang H Y, Wang S J, Chen S H and Chen C C 2015 *J. Alloys Compd.* **637** 30
[6] Xu H P, Wang R W, Wei D and Zeng C 2015 *J. Magn. Magn. Mater.* **385** 326
[7] Wang J, Wu Z and Li G 2015 *Mater. Sci. Eng. B* **201** 79
[8] Peng Y D, Nie J W, Zhang W J, Ma J, Bao C X and Cao Y 2016 *J. Magn. Magn. Mater.* **399** 88
[9] Zhong X X, Chen J C, Wang L, Li B J and Li L Z 2018 *J. Alloys Compd.* **735** 1603

[10] Lai J M, Xiao L K, Xiong Z W, Fang L M, Zhu W K, Kuang F G and Gao Z P 2023 *RSC Adv.* **13** 15892
[11] Wang J, Liu X, Li L and Mao X H 2012 *J. Cent. South Univ.* **28** 1266
[12] Guo R D, Yu G L, Zhu M M, Qiu Y, Wu G H and Zhou H M 2022 *J. Alloys Compd.* **895** 162724
[13] Kang E Y and Chung Y H 2009 *IEEE Trans. Magn.* **45** 2597
[14] Luo H, Wang X, Song K and Yang J 2016 *J. Electron. Mater.* **45** 4202
[15] Shokrollahi H, Janghorban K and Mazaleyrat F 2009 *Mater. Chem. Phys.* **114** 588
[16] Yu H Y, Lai X X, Zhong X C, Liu Z W, Guo B C, Chen X and Han G Z 2023 *Mater. Chem. Phys.* **303** 127765
[17] Hsiang H I, Wang S K and Chen C C 2020 *J. Magn. Magn. Mater.* **514** 167151
[18] Zhu Z Q, Wang P, Liu J Q, Lan P, Pang J and Zhang J Q 2023 *Magn. Magn. Mater.* **588** 171413
[19] Woo H J, Ahn J H, Kim C P, Choi D H, Kim S and Lee B W 2022 *J. Non-Cryst. Solids* **577** 121309
[20] Schubert D W, Werner S, Hahn I and Solovieva V 2019 *Compos. Sci. Technol.* **04** 26
[21] Taghvaei A H, Shokrollahi H, Janghorban K and Abiri H 2009 *Mater. Des.* **30** 3989
[22] Shokrollahi H and Janghorban H 2007 *J. Mater. Process. Technol.* **189** 1
[23] Pontes G, Schneider R, Senesi G S and Nicolodelli G 2024 *J. Non-Cryst. Solids* **627** 122814
[24] Neamţu B V, Geoffroy O, Chicinaş I and Isnard O 2012 *Mater. Sci. Eng. B* **177** 661
[25] Zhou B, Dong Y Q, Chi Q, Zhang Y Q, Chang L, Gong M G, Huang J J, Pan Y and Wang X M 2020 *Ceram. Int.* **46** 13449
[26] Wu S D, Dong Y Q, Li X B, Gong M J, Zhao R L, Gao W, Wu H, He A, Li J W, Wang X M and Liu X C 2022 *Ceram. Int.* **48** 22237
[27] Wang L L, Qiao L, Zheng J, Cai W, Ying Y, Li W C, Che S L and Yu J 2018 *J. Magn. Magn. Mater.* **452** 210
[28] Geng K J, Xie Y Y, Yan L and Yan B 2017 *J. Alloys Compd.* **718** 53
[29] Lei J, Zheng J W, Zheng H D, Qiao L, Ying Y, Cai W, Li W C, Yu J, Lin M and Che S L 2019 *J. Magn. Magn. Mater.* **472** 7
[30] Wang F L, Dong Y Q, Chang L, Pan Y, Chi Q, Gong M J, Li J W, He A and Wang X M 2021 *J. Solid State Chem.* **304** 122634
[31] Beijing Seven Star Flight Electronics Co. FeSi Powder Cores Performance Data.
[32] MAGNETICS, FeSi Powder Cores Performance Data
[33] Chang Sung Corporation, FeSi Powder Cores Performance Data
[34] Zhejiang Dongmu Keda Magnetic Electric Co., Ltd. FeSi Cores Performance Data.
[35] Zhao R L, Dong Y Q, Wu S D, Li X B, Liu Z H, Jia X J, Liu X, Wu H, Gao W, He A J and Li J W 2023 *Adv. Powder Technol.* **34** 103952
[36] Wang Y, Jing Y L, Wang P, Li Y X, Lu Q H and Tang X L 2020 *J. Magn. Magn. Mater.* **514** 167182